J|A|C|S
ARTICLES
Published on Web 10/27/2005

Regulation of Saccharide Binding with Basic Poly(ethynylpyridine)s by H^+-Induced Helix Formation

Hajime Abe,* Nozomi Masuda, Minoru Waki, and Masahiko Inouye*

Contribution from the Faculty of Pharmaceutical Sciences, Toyama Medical and Pharmaceutical University, Toyama 930-0194, and PRESTO, Japan Science and Technology Agency (JST), Saitama 332-0012, Japan

Received June 22, 2005; E-mail: abeh@ms.toyama-mpu.ac.jp (H.A.)

Abstract: A basic host polymer exhibiting pH-regulatable saccharide recognition has been investigated. Poly(*m*-ethynylpyridine) bearing dialkylamino groups forms helical complexes with saccharides to show induced circular dichroism (ICD). When trifluoroacetic acid was titrated on these complexes, the ICD was gradually enhanced until the amount of the acid reached ca. 0.5 molar equivalence versus the pyridine rings in the polymer, and further addition of the acid suppressed the ICD. The proper addition of the acid also increased the binding constants between the polymer and saccharides. These findings would be due to stabilization of the helical structure consisting of cisoid conformations for each of the adjacent pyridine pairs, which were caused by half-protonation of the pyridine rings. Computational analyses indicated that the pyridinium−pyridine dimeric structure prefers its cisoid conformation to its transoid one.

Introduction

As seen in many enzymes, recognition of substrates is often regulated by interaction with some chemical species (effectors) other than the substrates. Various kinds of effectors such as ions, ligands, and cofactors have been known to be involved in the working of enzymes.[1] In the chemistry of supramolecules, the regulation of their structures and functions has been regarded as one important subject. For mimicking biological processes by means of host−guest chemistry, it is essential to regulate the recognition ability and the structure of host molecules by external stimuli.[2−4] A proton is one of the most simple and ubiquitous chemical stimuli, and actually many kinds of enzymes are affected by a change of pH.[1] To regulate the higher order structure of artificial supramolecules, protonation has been utilized for conformational changes of hydrogen-bonding foldamers.[5,6] Protonation has also been applied to control the translocation of metal cations in ditopic azacrown and related host molecules.[7] So far, however, rare are such artificial host molecules that possess abilities to be regulated by their recognition strengths and higher order structures together with one kind of chemical stimulus.

Saccharides are one class of abundant substances in nature, and their recognition is still an interesting challenge in the field of molecular recognition.[8] Recently, during the course of our study about oligo- and polypyridine host molecules,[9,10] we found that *m*-ethynylpyridine polymers such as **1** associate with various saccharides to form helical complexes (Figure 1).[10−12] On those polymers, the pyridine nitrogen atoms behave as hydrogen-bonding acceptors to interact with the hydroxy groups of the guest saccharides. The rigid acetylene bridges arrange the pyridine rings at intervals fitting to the hydroxy groups of the guests, and the resulting multipoint hydrogen bondings induce the helix formation. The sense of the helices is biased by the chirality of the guest saccharides to show characteristic induced circular dichroism (ICD) at the wavelength range where the host

(1) Fersht, A. *Enzyme Structure and Mechanism*, 2nd ed.; W. H. Freeman and Co.: New York, 1985. Dixon, M.; Webb, E. C. *Enzymes*, 3rd ed.; Longman Group: London, 1979.
(2) Balzani, V.; Venturi, M.; Credi, A. *Molecular Devices and Machines − A Journey into the Nanoworld*; Wiley-VCH: Weinheim, Germany, 2003; pp 288−328. Lehn, J.-M. *Supramolecular Chemistry, Concepts and Perspectives*; VCH: Weinheim, Germany, 1995.
(3) A representive class of stimuli-regulatable host molecules is photoresponsive crown ethers. For reviews, see: Morrison, H., Ed. *Biological Applications of Photochemical Switches*; John Wiley & Sons: New York, 1993. Shinkai, S.; Manabe, O. *Top. Curr. Chem.* **1984**, *121*, 67−104. Shinkai, S. *Pure Appl. Chem.* **1987**, *59*, 425−430. Kimura, K.; Sakamoto, H.; Nakamura, M. *Bull. Chem. Soc. Jpn.* **2003**, *76*, 225−245. Cooke, G. *Angew. Chem., Int. Ed.* **2003**, *42*, 4860−4870.
(4) For recent examples of photoresponsive host molecules, see: Molard, Y.; Bassani, D. M.; Desvergne, J.-P.; Horton, P. N.; Hursthouse, M. B.; Tucker, J. H. R. *Angew. Chem., Int. Ed.* **2005**, *44*, 1072−75. Mulder, A.; Jukoviæ, A.; Huskens, J.; Reinhoudt, D. N. *Org. Biomol. Chem.* **2004**, *2*, 1748−1755. Mulder, A.; Jukoviæ, A.; van Leeuwen, F. W. B.; Kooijman, H.; Spek, A. L.; Huskens, J.; Reinhoudt, D. N. *Chem.—Eur. J.* **2004**, *10*, 1114−1123. Hunter, C. A.; Togrul, M.; Tomas, S. *Chem. Commun.* **2004**, 108−109. Goodman, A.; Breinlinger, E.; Ober, M.; Rotello, V. M. *J. Am. Chem. Soc.* **2001**, *123*, 6123−6214.
(5) (a) Dolain, C.; Maurizot, V.; Huc, I. *Angew. Chem., Int. Ed.* **2003**, *42*, 2737−2740. (b) Barboiu, M.; Lehn, J.-M. *Proc. Natl. Acad. Sci. U.S.A.* **2002**, *99*, 5201−5206.
(6) For a review introducing aromatic oligoamide foldamers including topics about their conformational control, see: Huc, I. *Eur. J. Org. Chem.* **2004**, 17−29.
(7) Lodeiro, C.; Parola, A. J.; Pina, F.; Bazzicalupi, C.; Bencini, A.; Bianchi, A.; Giorgi, C.; Masotti, A.; Valtancoli, B. *Inorg. Chem.* **2001**, *40*, 2968−2975. Amendola, V.; Fabbrizzi, L.; Mangano, C.; Pallavicini, P.; Perotti, A.; Taglietti, A. *J. Chem. Soc., Dalton Trans.* **2000**, 185−189. Ji, H.-F.; Dabestani, R.; Brown, G. M. *J. Am. Chem. Soc.* **2000**, *122*, 9306−9307. Ikeda, A.; Tsudera, T.; Shinkai, S. *J. Org. Chem.* **1997**, *62*, 3568−3574.
(8) Penadés, S. Ed. *Host-Guest Chemistry—Mimetic Approaches to Study Carbohydrate Recognition*; Topics in Current Chemistry 218; Springer-Verlag: Berlin, 2002. Davis, A. P.; Wareham, R. S. *Angew. Chem., Int. Ed.* **1999**, *38*, 2978−2996.
(9) Inouye, M.; Chiba, J.; Nakazumi, H. *J. Org. Chem.* **1999**, *64*, 8170−8176. Inouye, M.; Takahashi, K.; Nakazumi, H. *J. Am. Chem. Soc.* **1999**, *121*, 341−345. Inouye, M.; Miyake, T.; Furusyo, M.; Nakazumi, H. *J. Am. Chem. Soc.* **1995**, *117*, 12416−12425.
(10) Inouye, M.; Waki, M.; Abe, H. *J. Am. Chem. Soc.* **2004**, *126*, 2022−2027.

10.1021/ja054134u CCC: $30.25

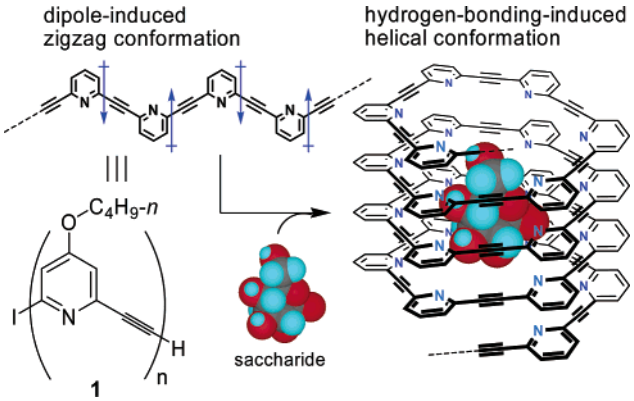

Figure 1. Structure of poly(*m*-ethynylpyridine) **1** and its conformation change induced by complexation with a saccharide guest (butoxy groups were omitted).

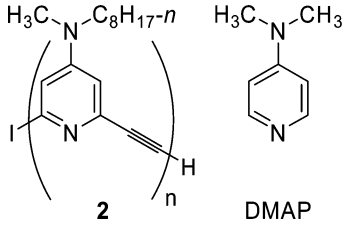

Figure 2. Structures of basic poly(*m*-ethynylpyridine) **2** and DMAP.

polymers absorb. At this point, considering the basicity of the pyridine moieties in the polymers, one may remark on the possibility that protonation on the nitrogen atoms can alter the nature of the ring moieties. The conversion of pyridine into pyridinium will locally change the hydrogen-bonding and electric properties of the rings and eventually influence the higher order structures of the polymers. Herein we report the development of (4-dialkylamino-2,6-pyridylene)ethynylene polymer **2**, saccharide binding of which is regulated by H^+-induced stabilization of the helical conformation (Figure 2).

Results

Molecular Design for Basic Poly(*m*-ethynylpyridine) 2. We have expected that protonation would be effective for the regulation of the properties and the structures for poly(*m*-ethynylpyridine)s. However, we were afraid that the basicity of polymer **1** was not high enough to capture many protons on the pyridine sites quantitatively. As protons are added one by one to the polymer, the basicity of the intermediate conjugate acids of the polymer becomes weaker. Therefore, one must use a large excess amount of acid, which may behave as an inhibitor for the hydrogen bonding between the polymer and saccharides. To make clear the influences of the protonation on poly(*m*-ethynylpyridine)s, rather higher basicity is required for the pyridine moieties. Thus, we decided to develop a highly basic poly(*m*-ethynylpyridine) by introducing dialkylamino groups to each pyridine ring on the polymer.

Among a variety of pyridine derivatives, one of the well-known compounds for its high basicity is 4-(dimethylamino)-pyridine (DMAP), which is often utilized as a catalyst in organic syntheses.[13] This utility is largely due to the virtue of the dialkylamino group that can stabilize the cationic conjugate acids and electrophile adducts of the pyridine ring. For the design of new highly basic polymer **2**, we anticipated that the adoption of a DMAP-like unit structure gives new properties and functions of the polymer. Recently, Heemstra and Moore et al. studied pyridine-containing *m*-phenylene ethynylene oligomers, which showed interesting features due to the helix stabilization by *N*-protonation or -methylation.[14]

In the molecular structure of **2**, the DMAP-like 4-(*N*-methyl-*N*-octylamino)pyridine units work as the centers for hydrogen bonding and the octyl chains improve the solubility of the polymer in organic media. The DMAP-like units are expected to be quantitatively protonated by treatment with the proper acid to alter the characteristics of **2**. The protonation of pyridine into pyridinium (1) converts the hydrogen-bonding mode of the ring from acceptor to donor, (2) gives a cationic nature to the ring, and (3) inverts the direction of the local dipole moment on the ring. As a result, the supramolecular characteristics of polymer **2**, e.g., the recognition ability for saccharides and the higher order structure of the complex, will be affected.

Preparation of Basic Polymer 2. The targeted basic polymer **2** was prepared mainly by repeating the Sonogashira reaction as shown in Scheme 1. To obtain a clean polymer of enough length, trimer **11** was chosen as the synthetic unit for polymerization. First, commercially available 2,6-dibromopyridine (**3**) was converted into 2,6-dibromo-4-nitropyridine (**4**) by the procedure in the literature.[15] The electron-deficient **4** was treated with *N*-methyloctylamine to give 2,6-dibromo-4-(*N*-methyl-*N*-octylamino)pyridine (**5**). Sonogashira reaction of **5** with excess (trimethylsilyl)acetylene yielded **6**, and the following protiodesilylation afforded diethynylpyridine **7**. On the other hand, copper-mediated halogen exchange[16] of **5** gave diiodopyridine **8**. Diiodo trimer **9** was obtained by a coupling reaction using **7** and an excess amount of **8**. Sonogashira reaction using (trimethylsilyl)acetylene and an excess amount of **9** gave **10**, and the following protiodesilylation yielded **11**, which was applied to the final polymerization to **2**. Before the protiodesilylation of **10**, the copper salt must surely be removed by washing with aqueous 1,2-diaminoethane; otherwise Glaser coupling leads to a byproduct diyne. For the polymerization to **2**, a diluted solution of **11** in DMF/*i*-Pr_2NH was treated under the Sonogashira reaction conditions to afford a crude mixture containing **2** after

(11) For reviews on helical foldamers and polymers, see: Hill, D. J.; Mio, M. J.; Prince, R. B.; Hughes, T. S.; Moore, J. S. *Chem. Rev.* **2001**, *101*, 3893−4011. Nakano, T.; Okamoto, Y. *Chem. Rev.* **2001**, *101*, 4013−4038. Cornelissen, J. J. L. M.; Rowan, A. E.; Nolte, R. J. M.; Sommerdijk, N. A. J. M. *Chem. Rev.* **2001**, *101*, 4039−4070. Schmuck, C. *Angew. Chem., Int. Ed.* **2003**, *42*, 2448−2452. See also ref 6. For artificial oligohydrazide foldamers which recognize saccharides, see: Hou, J.-L.; Shao, X.-B.; Chen, G.-J.; Zhou, Y.-X.; Jiang, X.-K.; Li, Z.-T. *J. Am. Chem. Soc.* **2004**, *126*, 12386−12394.

(12) Oligo(*m*-ethynylpyridine) derivatives are known to form double- or triple-stranded helicates by complexing with a Cu(I) or Ag(I) ion. See: Kawano, T.; Nakanishi, M.; Kato, T.; Ueda, I. *Chem. Lett.* **2005**, *34*, 350−351. Kawano, T.; Kato, T.; Du, C.-X.; Ueda, I. *Tetrahedron Lett.* **2002**, *43*, 6697−6700. Orita, A.; Nakano, T.; An, D. L.; Tanikawa, K.; Wakamatsu, K.; Otera, J. *J. Am. Chem. Soc.* **2004**, *126*, 10389−10396. Orita, A.; Nakano, T.; Yokoyama, T.; Babu, G.; Otera, J. *Chem. Lett.* **2004**, 1298−1299. Potts, K. T.; Horwitz, C. P.; Fessak, A.; Keshavarz-K, M.; Nash, K. E.; Toscano, P. J. *J. Am. Chem. Soc.* **1993**, *115*, 10444−10445.

(13) Spivey, A. C.; Arseniyadis, S. *Angew. Chem., Int. Ed.* **2004**, *43*, 5436−5441. Murugan, R.; Scriven, E. F. V. *Aldrichimica Acta* **2003**, *36*, 21−27. Grondal, C. *Synlett* **2003**, 1568−1569. Scriven, E. F. V. *Chem. Soc. Rev.* **1983**, *12*, 129−162. Höfle, G.; Steglich, W.; Vorbrüggen, H. *Angew. Chem., Int. Ed. Engl.* **1978**, *17*, 569−583. Shinkai, S.; Tsuji, H.; Hara, Y.; Manabe, O. *Bull. Chem. Soc. Jpn.* **1981**, *54*, 631−632.

(14) (a) Heemstra, J. M.; Moore, J. S. *J. Org. Chem.* **2004**, *69*, 9234−9237. (b) Heemstra, J. M.; Moore, J. S. *Chem. Commun.* **2004**, 1480−1481. (c) Heemstra, J. M.; Moore, J. S. *J. Am. Chem. Soc.* **2004**, *126*, 1648−1649. (d) Goto, H.; Heemstra, J. M.; Hill, D. J.; Moore, J. S. *Org. Lett.* **2004**, *6*, 889−892. (e) Heemstra, J. M.; Moore, J. S. *Org. Lett.* **2004**, *6*, 659−662.

(15) Neumann, U.; Vögtle, F. *Chem. Ber.* **1989**, *122*, 589−591.

(16) Suzuki, H.; Kondo, A.; Inouye, M.; Ogawa, T. *Synthesis* **1986**, 121−122.

Scheme 1. Preparation of Basic Poly(*m*-ethynylpyridine) **2**

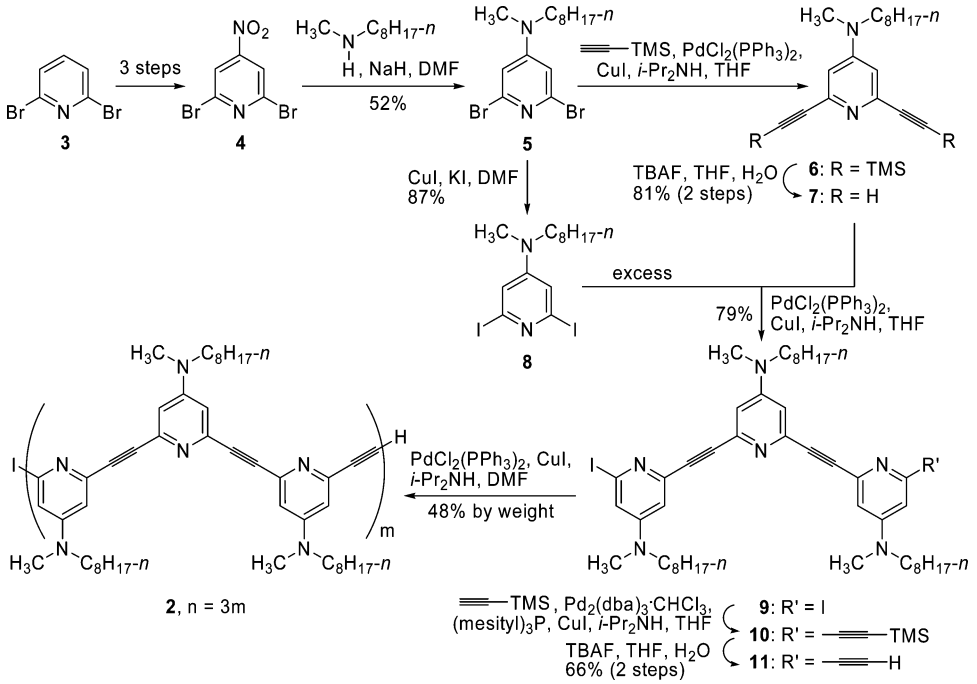

evaporation. The basicity of **2** was too high to be purified by preparative GPC; therefore, a considerable amount of **2** was adsorbed on the polystyrene gel. After several attempts, the centrifugal procedure was chosen for the purification of **2**. Thus, the crude mixture was dispersed into AcOEt, and the resulting brown precipitate was collected by centrifugation. By repeating this washing, the impurities were removed, judging from the ^{1}H NMR observation. The purified precipitate of **2** was applied to the experiments described below.

Molecular Weight, Optical Properties, and Concentration Dependency of Polymer 2. Vapor pressure osmometry (VPO) analyses for $CHCl_3$ solutions of **2** (ca. 1.2×10^{-2} to 2.0×10^{-3} mmol kg^{-1}, unit concentration) at 40 °C gave an M_n value of 1.1×10^4, which corresponds to the weight of the 45-mer, approximately.

The optical properties of **2** were studied by using CH_2Cl_2 or $CHCl_3$ as a solvent. The UV−vis spectrum of **2** in CH_2Cl_2 (Figure S1A in the Supporting Information; see also the red-colored spectrum in Figure 3A) exhibited a broad absorption band at $\lambda_{max} = 291$ nm with a shoulder around 310 nm. When the concentration of **2** was varied from 1.0×10^{-3} to 5.0×10^{-5} M (unit concentration), the shape of the spectrum did not show any meaningful change, and the absorbance at 291 nm obeyed Beer's law (Figure S1B). To examine the VPO conditions described above, absorbance at 363 nm was similarly plotted versus the concentration of **2** ranging from 1.0×10^{-1} to 3.9×10^{-4} M (unit concentration) in $CHCl_3$ at 40 °C, and obedience to Beer's law was also observed (Figure S1C). These linearities mean that the contribution of intermolecular π-interaction is negligible between two or more ground-state

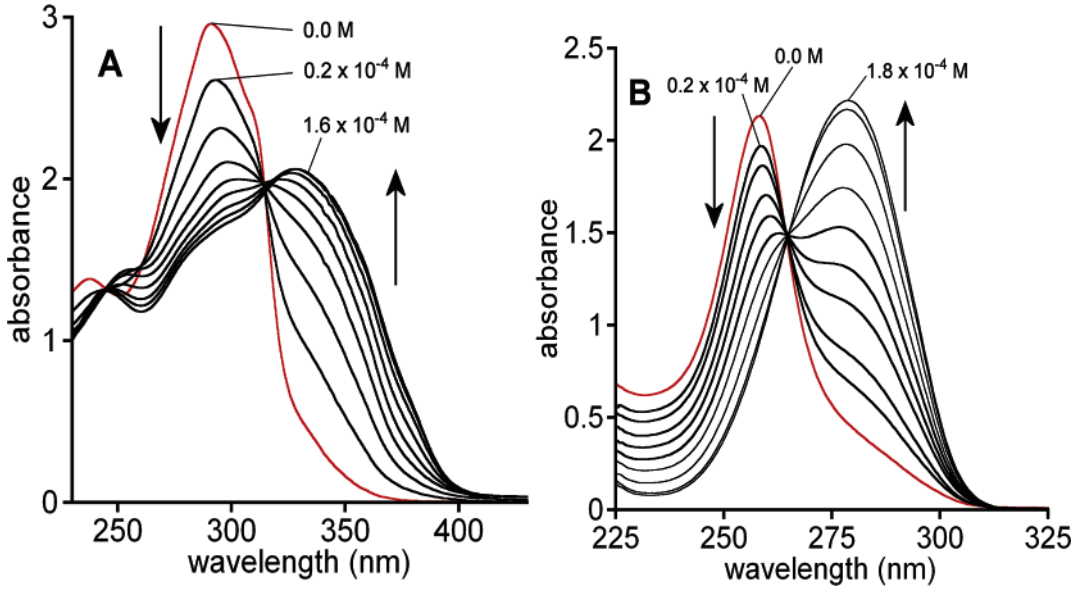

Figure 3. (A) Change of the UV−vis spectrum of **2** on titration with TFA. Conditions: [**2**] = 1.0×10^{-4} M (unit concentration), [TFA] = 0.0 to 1.6×10^{-4} M, CH_2Cl_2, 26 °C. Light path length 10 mm. (B) Change of the UV−vis spectrum of DMAP on titration with TFA. Conditions: [DMAP] = 1.0×10^{-4} M, [TFA] = 0 to 1.8×10^{-4} M, CH_2Cl_2, 26 °C. Light path length 10 mm. Red-colored lines represent the spectra in the absence of TFA.

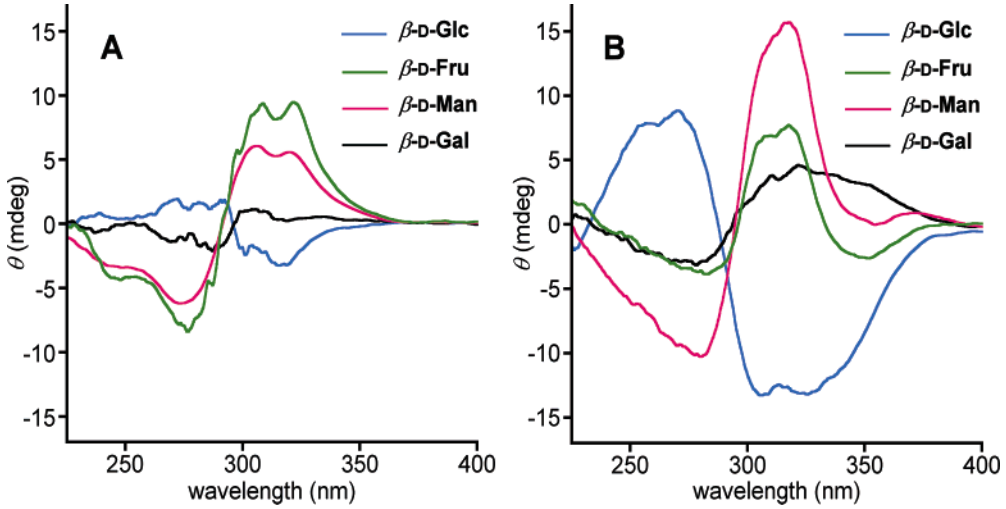

Figure 4. CD spectra of the complex between **2** (1.0 mM, unit concentration) and hexoses (2.5 mM) in CH_2Cl_2 in the (A) absence or (B) presence of TFA (0.5 mM) at 26 °C. Light path length 1 mm.

molecules of **2** up to 1.0×10^{-1} M. Thus, the relatively large M_n value based on the VPO analyses would not be due to self-association.

Fluorescence spectra of **2** in CH_2Cl_2 showed a structureless emission band at $F_{max} = 406$ nm accompanied by a broad weaker band around 580 nm on excitation at 315 nm (Figure S2 in the Supporting Information). A similar broad emission at a longer wavelength has also been observed in the case of **1**.[10] In the analyses of **2** under various concentrations, linear relationships were observed below 2.5×10^{-5} M (unit concentration) between the concentration and the fluorescence intensity at both 406 and 580 nm. Over that concentration, the intensities at both of the wavelengths deviated from the linearity probably because of intermolecular interaction between excited- and gound-state molecules of **2**. Considering this linearity, the emissive band at longer wavelength would be attributed to intramolecular excimer-like interaction, at least under a concentration below 2.5×10^{-5} M.

Spectral Changes of Polymer 2 on Addition of TFA. To study the characteristics of **2** as a strong polybase, the polymer was titrated with trifluoroacetic acid (TFA). As shown in Figure 3A, the UV−vis spectrum of **2** (1.0×10^{-4} M in CH_2Cl_2, unit concentration) significantly changed shape with the addition of TFA, and this spectral change almost ceased when the amount of TFA reached a small excess (1.5×10^{-4} M) relative to the amount of the pyridine units on **2**. During the titration, an isosbestic point was observed at 315 nm. A titration experiment was also carried out for DMAP itself (Figure 3B), and the UV−vis spectrum changed in a manner similar to that for **2**. In Figure 3B, the existence of an isosbestic point at 264 nm means the participation of just two kinds of absorptive species during the titration, DMAP and its conjugate acid. However, for polybase **2**, the observation of an isosbestic point in Figure 3A seems strange because there are many basic pyridine units in **2** and uncountable kinds of possible conjugate acids. It can be rationalized by the postulation that the π-conjugated systems in **2** and its conjugate acids are not linked smoothly through the "*meta*"-connection on the pyridine and pyridinium rings, so that each of the rings apparently behaves as an isolated chromophore to show the isosbestic point during the titration.

A titration experiment with TFA was also examined for **1** (1.0×10^{-4} M, unit concentration) as shown in Figure S3 in the Supporting Information. Although the shape of the UV−vis spectrum changed in a manner similar to the case of **2**, a rather excess amount of TFA, about 1.0×10^{-3} M, was needed to reach the end of this spectral change. This difference of sensitivities for TFA obviously comes from the difference of the Brønsted basicities of **1** and **2**. These findings demonstrated that **2** is more favorable to study the influences of protonation on the natures of poly(*m*-ethynylpyridine)s, especially on the association with saccharides by hydrogen bonds, which will be disturbed in the presence of a large excess of acid. Moreover, alkyl glycosides used as soluble guest saccharides in organic media might be decomposed by the extra acid.

When ^{1}H NMR spectra were measured for **2** (1.0×10^{-3} M) with and without TFA (0, 0.5×10^{-3}, and 1.0×10^{-3} M) in $CDCl_3$, it was found that protonation caused broadening and a downfield shift of the signals in **2** (see the Supporting Information). On the other hand, the changes of the chemical shifts were relatively small during further addition of TFA (up to 2.0×10^{-3} M), probably because the protonation on DMAP-like units in **2** was almost saturated by the addition of 1.0×10^{-3} M TFA. The ^{1}H NMR data also illustrated that the basicity of **2** is high enough for **2** to be a H^+-responsive poly(ethynylpyridine).

Association of Polymer 2 with Hexoses and Induced CD. As mentioned in our previous paper,[10] the butoxy-derived polymer **1** can associate with various saccharides to form helical complexes which show characteristic ICDs. Also for the cases of the basic polymer **2** (1.0 mM, unit concentration) in CH_2Cl_2 (Figure 4A), similar ICDs appeared when the polymer was treated with four kinds of hexoses (2.5 mM; see Chart 1), octyl β-D-glucopyranoside (***β*-D-Glc**), octyl β-D-fructopyranoside (***β*-D-Fru**), octyl β-D-mannopyranoside (***β*-D-Man**), and octyl β-D-galactopyranoside (***β*-D-Gal**). Under the presence of 0.5 mM TFA (the reason for this amount will be discussed later), the ICDs were somewhat enhanced (Figure 4B). These ICDs are similar to those for **1**[10] in that a main characteristic ICD band was observed around 300−350 nm due to the helical complex between the polymer and the guest hexose. Regardless of the presence or absence of TFA, **2** gave the main ICD band of the same sign as that for **1**[10] by the complexation with the same hexose except the case with ***β*-D-Gal**. The similarity of ICDs between **1** and **2** would reflect the similarity of the helical

Chart 1. Guest Hexoses

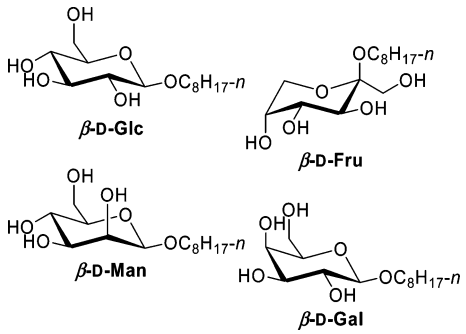

structures of the complexes. In the presence of TFA, it seems that a new shoulder of ICD appeared over 350 nm in the cases of **β-D-Glc** and **β-D-Gal**, but detailed reasons are obscured. It might suggest the contribution of two or more styles of helical structures.[17]

Titration with TFA on the Complex of Polymer 2 and Hexoses. As described above, addition of TFA affects the various optical natures of the basic polymer **2** and its complexes with hexoses. Quantitative studies were performed to shed light on the relation between the ICDs and the equivalency of added TFA. When TFA was titrated into a mixture of **2** (1.0 mM, unit concentration) and **β-D-Glc** (2.5 mM) in CH_2Cl_2, interesting transitions were observed in the CD spectra (Figure 5). At the initial stage of the titration, the ICD was gradually enhanced until 0.3 mM TFA was added. While a further amount of TFA was added up to 0.6 mM, only small structural changes were observed in the ICD. When the amount of TFA increased to 2.0 mM, the ICD began to diminish and finally disappeared. The highest ellipticity was observed at 326 nm in the presence of 0.3 mM TFA. For **β-D-Fru**, **β-D-Man**, and **β-D-Gal** as a guest hexose, the corresponding titration experiments with TFA exhibited similar behaviors of the ICD as shown in Figure S4 in the Supporting Information. Also in those cases, the highest ellipticities were observed when 0.3−0.5 mM TFA was added, and these ICDs were finally quenched by the addition of 1.3−2.0 mM TFA. Considering these results, when the unit concentration of **2** was 1.0 mM, we chose 0.5 mM as the amount of the additive TFA in the following experiments using hexoses as a titrant (see also the above and Figure 4B). This amount corresponds to a 0.5 molar equivalence for the pyridine rings on **2**, and approximately half-protonation is expected.

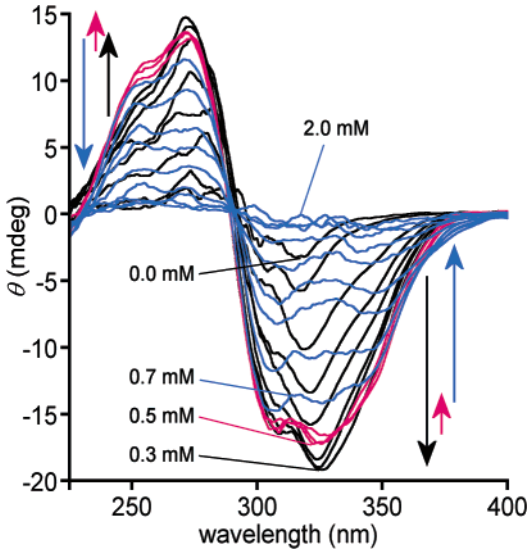

Figure 5. Change of the CD spectrum of the complex between **2** and **β-D-Glc** on titration with TFA. Conditions: [**2**] = 1.0 mM (unit concentration), [**β-D-Glc**] = 2.5 mM, [TFA] = 0−0.3 mM (black), 0.4−0.6 mM (red), 0.7−2.0 mM (blue), CH_2Cl_2, 26 °C. Light path length 1 mm.

The butoxy-derived polymer **1** (1.0 mM, unit concentration) in CH_2Cl_2 was also subjected to the titration with TFA in the presence of **β-D-Glc** (2.5 mM). However, the metamorphosis of the ICD was too complicated to make quantitative analyses, and the ICD did not disappear until 13 mM TFA was added (Figure S5 in the Supporting Information). In comparison with the case of **2**, this confusing observation for the ICD of **1** with **β-D-Glc** would be due to the weaker basicity of **1**, which was once found by UV−vis observation as shown in Figure S3. Thus, the higher basicity of **2** was corroborated to be favorable for quantitative studies on the influence of protonation on its higher order structure and saccharide recognition ability.

Binding Constants of Polymer 2 with Hexoses and the Additive Effects of TFA. To precisely evaluate the recognition abilities and effects of protonation, titrations for **2** with guest hexoses were performed. At first, the changes in the CD spectra of **2** in CH_2Cl_2 were pursued during the titration with **β-D-Glc** (Figure 6A), **β-D-Fru** (Figure S6A in the Supporting Information), or **β-D-Man** (Figure S7A in the Supporting Information) in the absence of TFA. In each of these titrations, growth of the ICDs was observed according to the addition of the hexose. The titration curves were drawn for the ellipticity at the corresponding wavelength of maximal ICDs as a function of the concentration of the hexoses added (Figures 6C, S6C, and S7C). From those curves, the formal binding constants were obtained as shown in Table 1 by iterative curve-fitting analyses based on the assumptions of 1:1 complexation between **2** and the hexoses[18] and a molecular weight of **2** of 1.1×10^4 (M_n from VPO analyses; see above). Among the three hexoses, **β-D-Glc**, **β-D-Fru**, and **β-D-Man**, the association of **2** with **β-D-Man** gave the strongest binding constant, $K_a = (3.3 \pm 0.5) \times 10^3$ M^{-1}. Since the deviations between the experimental and theoretical titration curves were small, the complexation in a 1:1 molar ratio of **2** and the guest hexose seems to be likely. Unfortunately, the titration with **β-D-Gal** gave only an insufficient result because of the weakness of the ICD as shown in Figure 4A.

As mentioned above, addition of TFA remarkably affected the association between **2** and hexose. In the presence of 0.5 mM TFA, the changes in the CD spectra of **2** (1.0 mM, unit concentration) were pursued during the titration with **β-D-Glc** (Figure 6B), **β-D-Fru** (Figure S6B), **β-D-Man** (Figure S7B), or **β-D-Gal** (Figure S8A in the Supporting Information) in CH_2Cl_2. The enhancement of the intensities of the ICDs by the presence of TFA was also observed in these quantitative experiments. The formal binding constants were obtained by curve-fitting analyses of the titration curves under the same assumptions as in the cases for the absence of TFA (Figures 6C, S6D, S7C, and S8B) and are summarized in Table 1. The formal binding constants of **2** with **β-D-Glc**, **β-D-Fru**, and **β-D-Man** in the presence of TFA are approximately 2−200 times as large as

(17) Stone, M. T.; Fox, J. M.; Moore, J. S. *Org. Lett.* **2004**, *6*, 3317−3320.
(18) For **1** (n = 24), the Job plot analysis indicated the 1:1 complexation with **β-D-Glc**.[10]

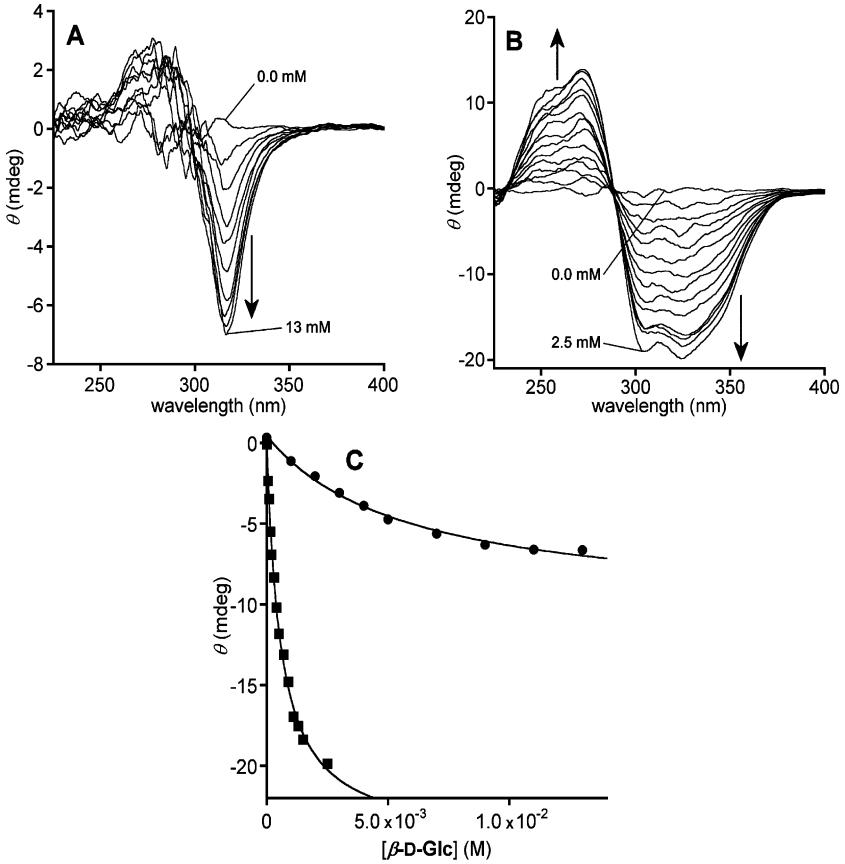

Figure 6. Change of the CD spectrum on the titration of **2** (1.0 mM, unit concentration) with ***β*-D-Glc** in CH_2Cl_2 at 26 °C in the (A) absence or (B) presence of TFA (0.5 mM). Light path length 1 mm. (C) Titration curves in the absence (circles; 315 nm was observed) or presence (squares; 324 nm was observed) of TFA. The lines are theoretical curves given by the iterative curve-fitting analyses assuming 1:1 complexation between **2** and ***β*-D-Glc** and a molecular weight of **2** of 1.1×10^4.

Table 1. Formal Binding Constants and $-\Delta G$ Values for the Association of Polymer **2** with Hexoses[a]

[TFA] (mM)	guest hexose	binding Constant K_a[b] (M^{-1})	$-\Delta G$ (kJ mol^{-1})
none	***β*-D-Glc**	$(1.7 \pm 0.3) \times 10^2$	13
0.5	***β*-D-Glc**	$(1.8 \pm 0.1) \times 10^3$	19
none	***β*-D-Fru**	$(1.0 \pm 0.1) \times 10^2$	11
0.5	***β*-D-Fru**	$(2.0 \pm 0.5) \times 10^4$	25
none	***β*-D-Man**	$(3.3 \pm 0.5) \times 10^3$	20
0.5	***β*-D-Man**	$(7.2 \pm 1.3) \times 10^3$	22
0.5	***β*-D-Gal**	$(2.2 \pm 0.4) \times 10^3$	19

[a] Conditions: [**2**] = 1.0 mM (unit concentration), [TFA] = 0 or 0.5 mM, CH_2Cl_2, 26 °C. See also the Figure 6 caption. [b] Obtained by curve-fitting analyses on the titration curves shown in Figures 6 and S6−S8.

those in the absence of TFA; thus, the addition of a proper amount of acid was found to improve the recognition abilities of **2** for saccharides.

Discussion

Equivalency of Added TFA. Scheme 2 shows one explanation for the observed additive effects of TFA on the association of **2** with saccharides. The direction of the local dipole moment on the pyridinium ring in **2** is postulated to be opposite that of the local dipole moment on the pyridine ring (see below). Taking the dipolar repulsion into account, the transoid conformation will be preferred in pyridine−pyridine and pyridinium−pyridinium pairs and the cisoid one will be preferred in the pyridinium−pyridine pair (Scheme 2, left). When the cisoid conformation lines up in **2** by the addition of TFA (0.5 molar equivalence versus the pyridine rings), a helical structure will spontaneously form. The resulting helix will be favorable for encompassing guest hexoses by multipoint hydrogen bondings. On the other hand, a sequence of the transoid conformation yields a zigzag structure, and its multipoint interaction with hexoses may suffer energetic loss resulting from the transformation of the transoid conformation into the cisoid conformation. Dipole-induced helical structures of heterocyclic strands were also reported by Lehn et al. for pyridine−pyrimidine and pyridine−pyridazine oligomers.[5b,19]

Apart from the local dipole moment, the hydrogen-bonding natures of pyridine and pyridinium moieties are different in that the former is a neutral hydrogen acceptor and the latter is a cationic donor. The electrostatic interaction of a cationic pyridinium proton with a hexose *O*H will be stronger than that of a neutral pyridine nitrogen with a hexose O*H*. The half-protonated helical complex between **2** and a hexose could be further stabilized by enforced stacking interactions as represented in Scheme 2 (right): the protonated pyridinium ring will interact with a

(19) For pyridine−pyrimidine oligomers, see: Barboiu, M.; Vaughan, G.; Kyritsakas, N.; Lehn, J.-M. *Chem.—Eur. J.* **2003**, *9*, 763−769. Gardinier, K. M.; Khoury, R. G.; Lehn, J.-M. *Chem.—Eur. J.* **2000**, *6*, 4124−4131. Ohkita, M.; Lehn, J.-M.; Baum, G.; Fenske, D. *Heterocycles* **2000**, *52*, 103−109. Ohkita, M.; Lehn, J.-M.; Baum, G.; Fenske, D. *Chem.—Eur. J.* **1999**, *5*, 3471−3481. Bassani, D. M.; Lehn, J.-M.; Baum, G.; Fenske, D. *Angew. Chem., Int. Ed. Engl.* **1997**, *36*, 1845−1847. Bassani, D. M.; Lehn, J.-M. *Bull. Chem. Soc. Fr.* **1997**, *134*, 897−906. Hanan, G. S.; Lehn, J.-M.; Kyritsakas, N.; Fischer, J. *J. Chem. Soc., Chem. Commun.* **1995**, 765−766. For pyridine−pyridazine oligomers: Cuccia, L. A.; Ruiz, E.; Lehn, J.-M.; Homo, J.-C.; Schmutz, M. *Chem.—Eur. J.* **2002**, *8*, 3448−3457. Cuccia, L. A.; Lehn, J.-M.; Homo, J.-C.; Schmutz, M. *Angew. Chem., Int. Ed.* **2000**, *39*, 233−237.

Scheme 2. Influences of Protonation on the Local Conformation (Left) and the Helical Structure (Right) of **2**

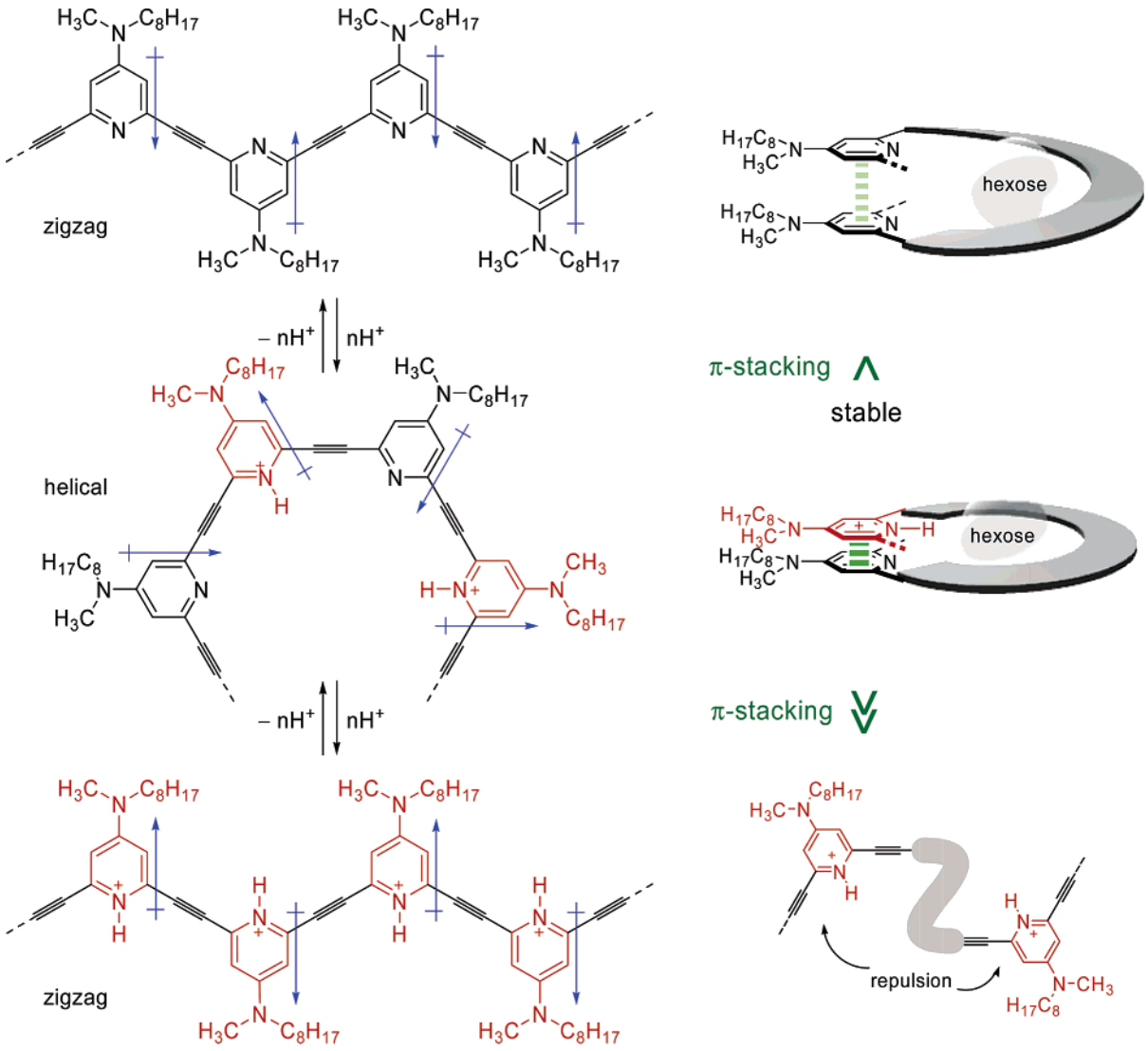

pyridine ring at an interval of one pitch by (cationic π)$-\pi$ stacking interaction,[14,20,21] which is more effective than (neutral π)$-\pi$ stacking expected in nonprotonated **2**. When most of the pyridine rings in **2** come to be protonated, electrostatic repulsion between the cationic centers may destabilize the helix. These hypotheses explain the observation that half-protonation of **2** is favorable for hexose recognition accompanying increased ICDs.

Computational Analyses for the Conformation of Polymer 2. The relative stabilities were computationally evaluated for cisoid and transoid conformations in the local structure in **2** and its conjugate acids. In advance, to select the proper structural formula of the conjugate acid, the stabilities were calculated

Chart 2. Calculated Dipole Moments for **12** and Its Conjugate Acids **12-H⁺-ring** and **12-H⁺-amino** and the Relative Stability Comparing the Two Acids

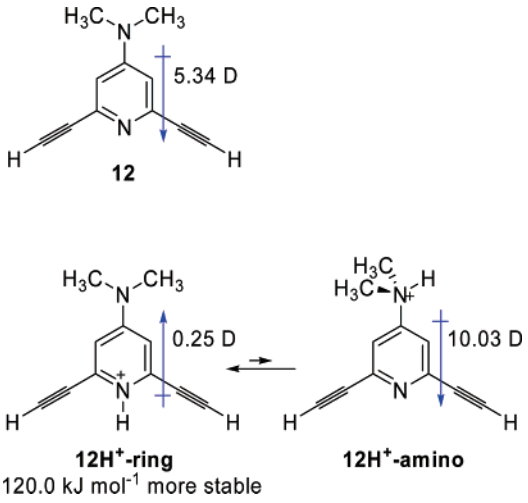

(20) For examples of π-interaction of pyridinium moieties, see: Hunter, C. A.; Low, C. M. R.; Vinter, J. G.; Zonta, C. *J. Am. Chem. Soc.* **2003**, *125*, 9936−9937. Priem, G.; Pelotier, B.; Macdonald, S. J. F.; Anson, M. S.; Campbell, I. B. *J. Org. Chem.* **2003**, *68*, 3844−3848. Hunter, C. A.; Low, C. M. R.; Rotger, C.; Vinter, J. G.; Zonta, C. *Proc. Natl. Acad. U.S.A.*, **2002**, *99*, 4873−4876. Yamada, S.; Morita, C. *J. Am. Chem. Soc.* **2002**, *124*, 8184−8185. Wisner, J. A.; Beer, P. D.; Drew, M. G. B. *Angew. Chem., Int. Ed.* **2001**, *40*, 3606−3609. Kawabata, T.; Nagato, M.; Takasu, K.; Fuji, K. *J. Am. Chem. Soc.* **1997**, *119*, 3169−3170. Kearney, P. C.; Mizoue, L. S.; Kumpf, R. A.; Forman, J. E.; McCurdy, A.; Dougherty, D. A. *J. Am. Chem. Soc.* **1993**, *115*, 9907−9919. McCurdy, A.; Jimenez, L.; Stauffer, D. A.; Dougherty, D. A. *J. Am. Chem. Soc.* **1992**, *114*, 10314−10321. Philp, D.; Slawin, A. M. Z.; Spencer, N.; Stoddart, J. F.; Williams, D. J. *J. Chem. Soc., Chem. Commun.* **1991**, 1584−1586. Ortholand, J.-Y.; Slawin, A. M. Z.; Spencer, N.; Stoddart, J. F.; Williams, D. J. *Angew. Chem., Int. Ed. Engl.* **1989**, *28*, 1394−1395. Petti, M. A.; Shepodd, T. J.; Barrans, R. E., Jr.; Dougherty, D. A. *J. Am. Chem. Soc.* **1988**, *110*, 6825−6840.

(21) For a review on cation$-\pi$ interaction, see: Ma, J. C.; Dougherty, D. A. *Chem. Rev.* **1997**, *97*, 1303−1324. See also: Klärner, F.-G.; Kahlert, B. *Acc. Chem. Res.* **2003**, *36*, 919−932.

Chart 3. Comparison of the Calculated Relative Stabilities for the Transoid (Left) and Cisoid (Right) Conformers of Dimer **13** and Its Conjugate Acids **13-1H**$^+$ and **13-2H**$^+$

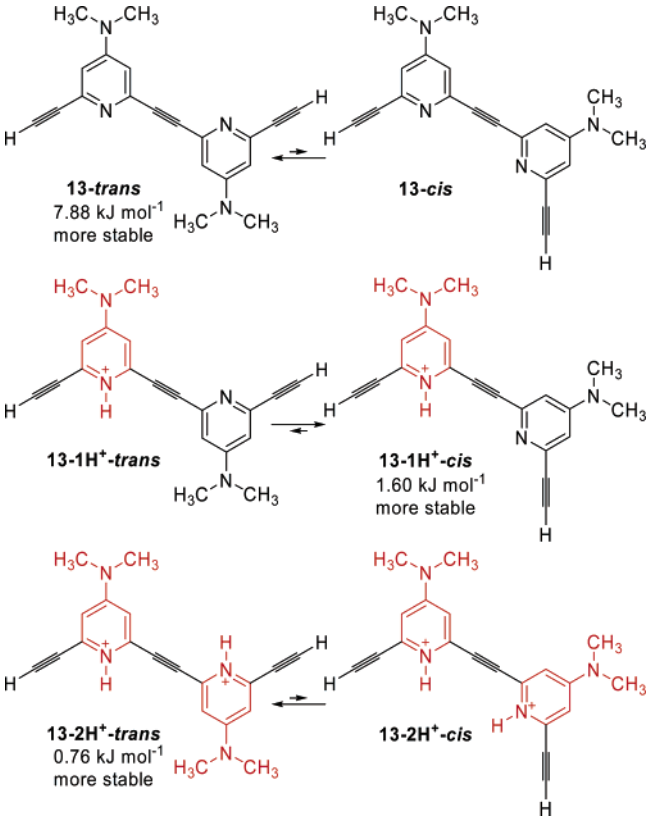

for two possible isomeric conjugate acids of a DMAP-like molecule, 2,6-diethynyl-4-(*N*,*N*-dimethylamino)pyridine (**12**) (Chart 2). One conjugate acid is **12-H**$^+$**-ring** protonated at 1-N in the ring, and the other is **12-H**$^+$**-amino** protonated at the dimethylamino nitrogen. The DFT calculations indicated that **12-H**$^+$**-ring** is much more stable than **12-H**$^+$**-amino** by 120 kJ mol^{-1}. Therefore, the protonation at the dialkylamino groups in **2** is regarded as a negligible process in the following computational studies. Furthermore, the calculation confirmed that the dipole moment on **12-H**$^+$**-ring** is reversed as compared to that on **12** (see above).

Next, the stabilities for transoid and cisoid conformations in **2** were computationally assessed by using bis[4-(*N*,*N*-dimethylamino)-6-ethynyl-2-pyridyl]ethyne (**13**) as a model dimeric structure. Both the transoid and cisoid conformers of **13** and its monoprotonated **13-1H**$^+$ and diprotonated **13-2H**$^+$ were submitted to DFT calculations using 6-31(d) basis sets for geometrical optimization and zero-point energy correction and 6-311+(2d,p) basis sets for single point analyses. The results are summarized in Chart 3. The calculation indicated that the cisoid conformer **13-1H**$^+$***-cis*** is more stable than the transoid conformer **13-1H**$^+$***-trans*** in the case of the pyridinium−pyridine dimer **13-1H**$^+$ whereas the transoid conformers are more stable for the pyridine−pyridine **13** and the pyridinium−pyridinium **13-2H**$^+$. These data support the discussion described above, and one may imagine that the preferable conformation of a pyridine−acetylene−pyridine repeat could be controlled by the degree of protonation. For polymer **2**, alternate half-protonation on its pyridine rings would stabilize the cisoid conformation at the local structure to help the formation of a helical higher order entity.

Conclusion

By repeating the Sonogashira reaction, *m*-ethynylpyridine polymer **2** bearing dialkylamino groups was synthesized. Polymer **2** has high basicity, being comparable to that of DMAP, and associates with hexoses to form helical complexes with characteristic ICDs. These ICDs and the binding constants were enhanced by the addition of trifluoroacetic acid of ca. 0.5 molar equivalence versus the pyridine rings on **2**, and further addition of the acid suppressed the ICDs. The half-protonation on **2** would stabilize the helical conformation probably with the aid of the preferable local cisoid conformation and the enforced intramolecular pyridinium−pyridine π-stacking. This preference for the cisoid conformation was supported by DFT calculations. The DMAP-like moieties in **2** are potentially expected to serve as catalysis centers, and that in combination with the recognition abilities will allow realization of artificial enzymes of a new type, a study now under way.

Acknowledgment. We gratefully acknowledge the Takeda Science Foundation for financial support.

Supporting Information Available: The entire Experimental Section, Figures S1−S8, ^{1}H NMR spectra for compounds **2**, **5**, **7**, **8**, **9**, and **11**, and the results of computational analyses for **12**, **13**, and their conjugate acids shown in Charts 2 and 3. This material is available free of charge via the Internet at http://pubs.acs.org.

JA054134U